Proc. Natl. Acad. Sci. USA
Vol. 93, pp. 5556–5561, May 1996
Genetics

Microfabricated structures for integrated DNA analysis

(PCR/silicon fabrication/thermocapillary pump)

MARK A. BURNS*†, CARLOS H. MASTRANGELO‡, TIMOTHY S. SAMMARCO*, FRANCIS P. MAN‡, JAMES R. WEBSTER‡, BRIAN N. JOHNSON§, BRADLEY FOERSTER*, DARREN JONES§, YAKEITHA FIELDS*, ADAM R. KAISER*, AND DAVID T. BURKE§¶

Departments of *Chemical Engineering, ‡Electrical Engineering and Computer Science, and §Human Genetics, †Bioengineering Program, and ¶Institute of Gerontology, University of Michigan, Ann Arbor, MI 48109

Communicated by Francis S. Collins, National Center for Human Genome Research, Bethesda, MD, December 29, 1995 (received for review December 13, 1995)

ABSTRACT **Photolithographic micromachining of silicon is a candidate technology for the construction of high-throughput DNA analysis devices. However, the development of complex silicon microfabricated systems has been hindered in part by the lack of a simple, versatile pumping method for integrating individual components. Here we describe a surface-tension-based pump able to move discrete nanoliter drops through enclosed channels using only local heating. This thermocapillary pump can accurately mix, measure, and divide drops by simple electronic control. In addition, we have constructed thermal-cycling chambers, gel electrophoresis channels, and radiolabeled DNA detectors that are compatible with the fabrication of thermocapillary pump channels. Since all of the components are made by conventional photolithographic techniques, they can be assembled into more complex integrated systems. The combination of pump and components into self-contained miniaturized devices may provide significant improvements in DNA analysis speed, portability, and cost. The potential of microfabricated systems lies in the low unit cost of silicon-based construction and in the efficient sample handling afforded by component integration.**

The recent rapid accumulation of genomic data for many organisms (1–3), together with the development of powerful DNA-based typing methods (4–6), has stimulated the demand for genetic information. The examination of the heritable components of common human diseases will involve population-based genetic studies and will require genetic typing of thousands of individuals at numerous genetic loci (7). To date, the labor- and material-intensive technologies for genetic typing have restrained its application to population analysis. Studies of large populations will benefit significantly from reductions in genotyping costs and improvements in equipment portability.

DNA analysis using PCR-amplified polymorphism has become a general method for biological and clinical research. The biochemistry of the assay is robust and virtually identical for any genetic locus or source organism. Although well characterized, PCR analysis has not been assembled into a simple automated system. Standard PCR-based DNA typing involves (*i*) liquid handling of reagent and DNA template solutions, (*ii*) measurement of solution volumes, (*iii*) mixing of reagent and template, (*iv*) controlled thermal reaction of the mixture, (*v*) loading of the sample to an electrophoresis gel, and (*vi*) detection of DNA products. The complete process relies on human intervention at several stages to transfer liquids, mix reagents, track reaction vessels, and analyze results. In the ideal case, the processing steps would be merged into a single, integrated system composed of modular devices that are fully compatible and that function with minimal operator interaction.

The publication costs of this article were defrayed in part by page charge payment. This article must therefore be hereby marked "*advertisement*" in accordance with 18 U.S.C. §1734 solely to indicate this fact.

Although there are many formats, materials, and size scales for constructing integrated fluidic systems, silicon and glass microfabricated devices can provide a general solution. Silicon micromachining is well established in commercial industry, has low incremental unit costs, and uses rapid, computer-based design technologies. These characteristics have led to its proposal as a candidate technology for the construction of high-throughput DNA analysis devices (8–10). As mechanical materials, both silicon and glass have well-known fabrication characteristics (11). To date, a number of devices have been micromachined, including pumps and valves (12–14), reaction chambers (8, 15), and separation and detection systems (6, 9, 16–20). Silicon and glass devices are economically attractive because the associated micromachining methods are, essentially, photographic reproduction techniques. Once a photographic template is generated, it can be used almost indefinitely to produce identical replicate structures.

We report the development and testing of a set of micromachined components for DNA analysis, as well as the preliminary integration of those components. The goal of this process is a minimal fully integrated device and would include the elements identified in Fig. 1. In the proposed format, sample and reagent are injected into the device through entry ports (Fig. 1*A*) and the solutions pumped through channels (Fig. 1*B*) to a thermally controlled reactor where mixing and restriction enzyme digestion or PCR amplification occurs (Fig. 1*C*). The biochemical products are then moved by the same pumping method to an electrophoresis channel (Fig. 1*D*) where DNA migration data are collected by a detector (Fig. 1*E*) and exported as electronic information. The core component of the system is a simple thermocapillary pump capable of connecting diverse individual elements.

MATERIALS AND METHODS

Heater Element Wafer Fabrication. Heater elements were made with a silicon wafer (p-type, 18–22 Ω-cm, ⟨100⟩, boron concentration $\approx 10^{15}$ cm^{-3}) as a substrate for growth of SiO_2 thermal oxide (1 μm). A photoresist (AZ-5214-E; Hoescht–Celanese) was applied to the wafer and spun at 3000 rpm for 30 sec. The resist was patterned using a mask (M1) and developed. Reactive ion etching (PlasmaTherm, St. Petersburg, FL) was performed to 0.35-μm depth into the SiO_2 layer at the following conditions: CHF_3, 15 standard cubic centimeters per minute (sccm); CF_4, 15 sccm; 4 mTorr; dc bias voltage of 200 V, 100 W, 20 min. The etch depth was measured by profilometer, and 0.35-μm metallic aluminum was electron beam deposited. The resist and overlying metal were lifted off by development using Microposit 1112A remover in solution (Shipley, Marlboro, MA). The barrier layers covering the aluminum elements consist of sequentially deposited 1 μm SiO_x, 0.25 μm Si_xN_y, and 1 μm SiO_x using plasma-enhanced

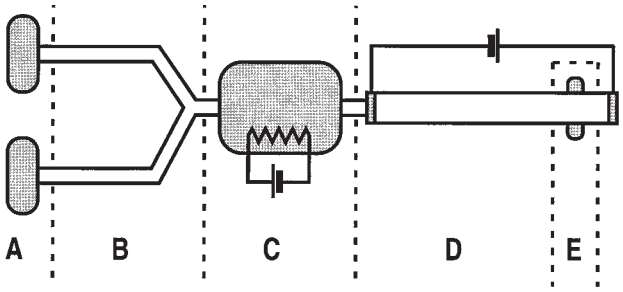

FIG. 1. Example of an integrated DNA analysis system, represented schematically. The individual components of the system are injection entry ports (*A*), liquid pumping channels (*B*), thermally controlled reaction chamber (*C*), electrophoresis channel (*D*), and DNA band migration detector (*E*). Each component would have associated sensors, control circuitry, and external connections.

chemical vapor deposition. Reactive ion etch was used to etch contact holes to the metal layer using a second mask (M2) with conditions: CHF_3, 15 sccm; CF_4, 15 sccm; 4 mTorr; and dc bias voltage of 200 V, 100 W, 120 min. Each heating element used as a temperature sensor was calibrated by measurement of electrical resistance at 22°C and 65°C under constant voltage; intermediate temperatures were estimated by linear interpolation.

Channel Wafer Fabrication. Channels were prepared on 500-μm-thick glass wafers (Dow Corning 7740) using standard aqueous-based etch procedures. The initial glass surface was cleaned and received two layers of electron beam-evaporated metal (20 nm chromium, followed by 50 nm gold). Photoresist (Microposit 1813) was spun at 4000 rpm for 30 sec, patterned using a mask (G1), and developed. The metal layers were etched in chromium etchant (Cr-14; Cyantek, Newark, CA) and gold etchant (Gold Etchant TFA; Transene, Rowley, MA) until the pattern was clearly visible on the glass surface. The accessible glass was then etched in a solution of hydrofluoric acid and water (1:1). Etch rates were estimated using test wafers, with the final etch giving channel depths of 20–30 μm. For each wafer, the depth of the finished channel was determined using a surface profilometer. The final stripping steps removed the remaining photoresist material (PRS-2000; J. T. Baker) and metal layers (Cr-14 and Gold Echant TFA).

Diffusion Diode Wafer Fabrication. Diode detectors were prepared on 200 Ω·cm, ⟨100⟩, boron-doped, *p*-type silicon wafer substrates. Diffused layers of phosphorus (5×10^{14} cm^{-2}) and boron (1×10^{15} cm^{-2}) were ion-implanted onto the sample in lithographically defined regions (mask D1); thermal silicon oxide was grown (0.2 μm at 900°C) over the wafer; and contact holes were etched to the diffusion layer with buffered hydrofluoric acid solution. A 3.3-μm layer of photoresist (Microposit 1400-37) was patterned to define the metal pads (mask D2); 50-nm chromium followed by 400-nm gold was evaporated over the resist; and the metallization lifted off the regions retaining the resist. In some initial radiation sensitivity tests, a layer of photoresist (Microposit 1813) was applied across the wafer and baked for 110°C for 30 min to form an aqueous solution barrier. Additional experiments used a double layer of plasma-enhanced chemical vapor deposition silicon oxide and silicon nitride as a barrier, similar to the layers described for the heater-element wafer. Radioactive phosphorus (^{32}P) decay events were detected using a sample of labeled DNA in PCR buffer placed on the barrier layer. To test sensitivity, the detector was connected to a charge-sensitive preamplifier (model 550A, EV-Products, Saxonburg, PA), followed by a linear shaping amplifier and a standard oscilloscope, and events were computer recorded.

Glass-to-Silicon Wafer Bonding and Channel Pretreatment. Channels etched on glass were bonded to the heater element wafer using a thin film of applied optical adhesive (SK-9 Lens Bond; Sumers Laboratories, Fort Washington, PA). The bond was cured under a UV light source (365 nm) for 12–24 h. Tests of cured adhesive samples indicated little or no inhibition of restriction endonuclease or thermostable DNA polymerase. Prior to each drop-motion experiment, the bonded channels were prepared by washing with ≈100 μl each of the following solutions in series: 0.1 M NaOH, 0.1 M HCl, 10 mM Tris·HCl (pH 8.0), deionized H_2O, Rain-X Anti-Fog (Unelko, Scottsdale, AZ), and bovine serum albumin at 500 μg/ml (restriction enzyme grade; GIBCO/BRL).

Drop Motion and Restriction Enzyme Digestion. The bonded channel device was placed on a stereoscope stage (Olympus SZ1145), and the contact pads for the heating elements were connected to a regulated power supply. Aqueous samples were applied to each of the Y-channel branches by gently touching a suspended drop to channel opening and allowing capillary action to draw the sample into the device. Measurements of drop length in the channel provided a visual check of the loaded volumes. Heating of the drops occurred by passing ≈30 V dc through the element in short pulses and observing the movement of the drops. A small detectable reduction in drop volume from evaporation was noted in each experiment, usually <30% of the initial drop length. Drop movement was recorded with a Hamamatsu (Middlesex, NJ) video camera on videotape, and still images were obtained from the videotape without modification.

For the restriction enzyme digestion of DNA, a drop containing 0.2 unit of *Taq* I restriction enzyme in reaction buffer (100 mM NaCl/10 mM $MgCl_2$/10 mM Tris·HCl, pH 8.0), 150 nl total volume was introduced into one branch of a Y-channel while a drop containing 150 nl of 0.1 μg of supercoiled plasmid per μl (Bluescript SK; Stratagene) was introduced into the other. Following drop motion, digestion occurred by holding the drop at a previously calibrated 65°C for 10 min using ≈4 V dc. The single channel portion of the device was uniformly heated by using seven contiguous heater elements, and the temperature was monitored by measuring electrical resistance. The electronic control system consisted of a National Instruments (Austin, TX) LabView controller and virtual instrument software operating on an Apple Macintosh 950.

Microfabricated Channel Gel Electrophoresis. Channels etched on glass (see Fig. 3*A*) were bonded to a quartz microscope slide using SK-9 optical adhesive and 24-h UV-illuminated curing. A 10% acrylamide electrophoresis mix (10% acrylamide/0.3% bis-acrylamide/89 mM Tris·HCl/89 mM sodium borate/10 mM EDTA/0.001% *N*,*N*,*N*′,*N*′-tetramethylethylenediamine/0.01% ammonium persulfate) was injected into the channel and allowed to polymerize. Following polymerization, the slide was immersed in a horizontal electrophoresis apparatus containing gel running buffer (89 mM Tris·HCl/89 mM sodium borate/10 mM EDTA). A 50-μl sample of 100 ng of DNA per μl (Bluescript SK plasmid digested with *Msp* I) containing 0.01% YOYO-1 dye (Molecular Probes) was placed at the negative electrode opening of the channel, and current was applied until a green fluorescing band appeared at the buffer-to-gel interface (12 V/cm, ≈2 min). The remaining DNA solution was rinsed away, replaced by running buffer, and electrophoresis was continued by applying current at 12 V/cm for 120 min. The gel was photographed under an incandescent light source and viewed using an Olympus stereo microscope and Nikon 35 mm camera with no filters.

PCRs on Silicon Wafer Surfaces. PCR was performed using standard buffer and primer concentration conditions for *Thermus aquaticus* DNA polymerase enzyme (4, 21). PCR temperature profiles were as follows: 94°C for 4 min, preincubation; 94°C for 1 min, 62°C for 1 min, 72°C for 1 min, 35 cycles; 72°C for 10 min, final extension. The primer set is specific for a portion of the mouse *Tfe3* locus and produces a 460-bp-amplified product (primer A, 5′-TAAGGTATGCCCCTGGCCAC-3′; primer B, 5′-AAGGTCAGCACAGAGTCCTCA-3′) (22). For each experimental run a complete 75-μl reaction

mixture was prepared using 100 ng of purified genomic mouse DNA as template and divided into three reactions of 25 μl each. The first reaction was maintained at room temperature for 2 h; the second was reacted in a thin-wall polypropylene tube under mineral oil and cycled in a standard thermal cycler; and the third was placed on the surface of the described heater wafer within a small polypropylene ring (4 mm diameter, 1.5 mm height) and covered with light mineral oil. Wafer temperatures were determined by measuring changes in heater element resistance and were controlled by a National Instruments LabView controller and software operating on an Apple Macintosh 950. On completion of the reactions, the three samples were examined for efficiency of amplification by agarose gel electrophoresis and ethidium bromide staining.

Capillary Gel Electrophoresis. Capillary gel electrophoresis of DNA samples was performed using a Beckman P/ACE instrument with a laser-induced fluorescence detector and 37 cm length, 100 μm diameter, linear polyacrylamide gel capillary according to manufacturer's recommendation. Samples were stained, then injected electrokinetically using a water-stacking procedure and run at 7400 V dc for 45 min.

RESULTS

Thermocapillary Pump. The thermocapillary pump provides movement of discrete drops in micron-sized channels with no moving parts or valves. A pumping system based on individual drop movement has three advantages for DNA analysis: (*i*) samples can be readily divided and mixed, (*ii*) the sample volume can be determined by measuring the drop length, and (*iii*) each sample is kept separate, reducing the risk of cross-contamination.

Motion of discrete liquid samples in micron-sized channels can be accomplished by differentially heating the drop interfaces (Fig. 2). In channels, a pressure difference occurs across the liquid–air interface (i.e., capillary pressure). The pressure difference, ΔP_c, is a function of the surface tension and, for rectangular channels, is given by

$$\Delta P_c = P_{atm} - P_{liquid} = (2\sigma\cos\theta)(1/h + 1/w), \qquad [1]$$

where θ is the contact angle, h is the channel height, w is the channel width, and σ is the liquid–vapor interfacial tension given by

$$\sigma = \sigma_o(1 - bT), \qquad [2]$$

where σ_o and b are positive constants and T is the temperature (23). Increasing the temperature on one end of the drop decreases the surface tension and, therefore, increases the internal pressure on that end. The pressure difference between the two ends pushes the drop towards the direction of lower pressure at a rate given by (ignoring edge effects, $h \ll w$)

$$\langle v\rangle = (h/6\mu L)[(\sigma\cos\theta)_a - (\sigma\cos\theta)_r], \qquad [3]$$

where μ is the viscosity, L is the length of the drop, and the subscripts a and r refer to the advancing and retreating interfaces, respectively. Note that contact angle hysteresis ($\theta_a \neq \theta_r$) requires a threshold pressure difference for positive motion (24, 25).

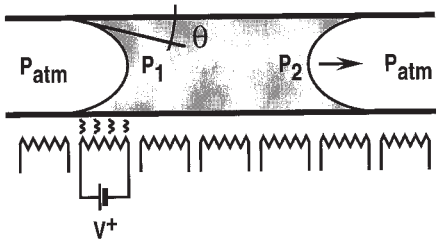

FIG. 2. Schematic drawing showing the principle of thermally induced drop motion in a closed channel. The case of a single aqueous drop in a hydrophilic channel is presented, where V is an applied voltage, P_{atm} is atmospheric pressure, P_1 is the receding-edge internal pressure, P_2 is the advancing-edge internal pressure, and θ is the contact angle of the liquid–gas–solid interface. The contact angle will depend on the surface characteristics of the channel and the constituents of the drop, with a hydrophilic interaction giving θ between 0 and 90 degrees, and a hydrophobic surface giving θ between 90 and 180 degrees. Surface treatments can also reduce contact angle hysteresis and, therefore, reduce the temperature difference necessary for drop motion.

A device capable of moving and mixing nanoliter drops using differential heating was constructed by bonding a surface-etched glass wafer to a silicon substrate. A standard aqueous acid etch is used to produce channels on the glass wafer having two parallel lanes merging into a single lane (a Y shape; Fig. 3*A*) with dimensions 500 μm wide and 25 μm deep. Metal heaters are patterned on the silicon substrate having the same Y format and are protected from liquid by a thin-film barrier (Fig. 3 *B* and *C*). The heaters are formed by using an inlay process to prevent defects in the barrier layer. The complementary heater and channel wafers are aligned and bonded with an adhesive to form the finished device.

Movement and Mixing of Liquid Samples. Samples were loaded into the two parallel channels (Fig. 4*A*); the hydrophilic surface of the channel allows the process to occur spontaneously. The drop volumes are ≈60 nl and are calculated from the drop length and the known channel cross section. Activating the heaters under the left interfaces propels the drops forward to the channel intersection where they meet and join to form a single larger drop (Fig. 4 *B* and *C*). The combined drop is stopped by turning off all heating elements (Fig. 4*D*) and can be reversed by heating the right interface. Additionally, circulation patterns generated in the drop during motion aid in mixing the liquid sample. Experiments using the metal elements as both heaters and temperature sensors demonstrate that a temperature differential of 20–40°C across the drop is sufficient to provide forward motion in this particular channel.

Other simple sample-handling operations can be performed with this device. For example, drop splitting can be accomplished in two ways. First, a drop can be moved from the single channel, past the Y-channel intersection, and into the two separate channels. While the motion of the drop is accomplished by heating the retreating interface, the amount of liquid that enters each of the two channels can be controlled by selectively heating one of the advancing interfaces. The drop will preferentially move into the less-heated branch channel. Alternatively, splitting can be performed on a drop held in a single channel by localized heating at the drop's center until a bubble of water vapor forms. Continued heating of the expanding water–vapor bubble propels the two drop-halves in opposite directions. Although an increased gas-phase pressure is responsible for this latter motion, properly placed air vents in the channel should allow the split drops to be moved independently using thermocapillary pumping.

To confirm compatibility of the propulsion system with DNA samples and enzymes, an integrated system was tested combining drop motion, sample mixing, and controlled thermal reaction (Fig. 1 *A–C*). A sample containing plasmid DNA (supercoiled BluescriptSK; Stratagene) was loaded into one branch of the Y channel, and a second sample containing *Taq* I restriction enzyme and digestion buffer was loaded into the other. After sample merging by thermocapillary pumping, the combined drop was maintained at 65°C for 10 min using the integral heaters and temperature sensors. Capillary gel electrophoresis of the reaction products confirmed that DNA digestion on the silicon device (Fig. 5*A*) was similar to reactions performed in a standard polypropylene vessel.

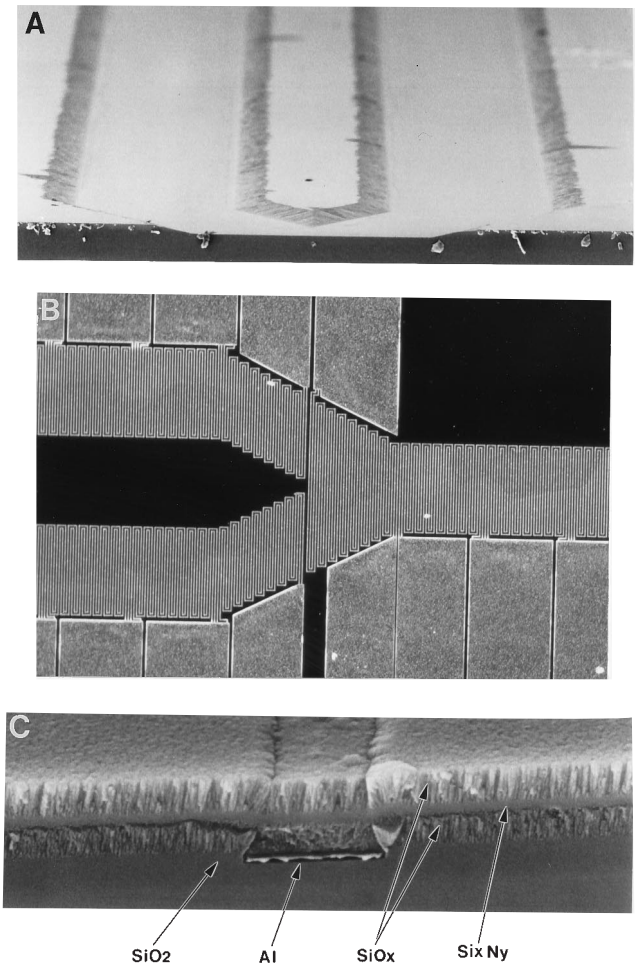

FIG. 3. Silicon and glass micromachined components for a thermocapillary pump. (*A*) Scanning electron micrograph of a channel formed in glass using a wet-etch process. The view shows the cross section and etched face of the wafer immediately adjacent to the intersection of two channels. The channels are constructed as two parallel lanes, each 500 μm wide and 25 μm deep, merging into one lane of the same cross-sectional dimensions. The channels were prepared on 0.5-mm thick glass wafers with standard aqueous-based etching procedures. (*B*) Photomicrograph of heater elements on the surface of a silicon wafer. The elements are designed to match the channel layout and are arrayed as two parallel lanes, each 500 μm wide, merging into one lane. The individual heaters consist of paired aluminum wires winding across a 500 $\times$ 500 μm region. The broad metal areas on either side of the elements are bonding locations for connection to external circuitry. (*C*) Scanning electron micrograph of a heater wire in cross section. The arrows indicate the deposited aluminum, silicon oxide, and silicon nitride layers. The plasma-enhanced chemical vapor deposition process for forming the silicon oxide and silicon nitride layers results in an undefined stoichiometry; therefore, the layers are designated SiO_x or Si_xN_y. The width of the aluminum element is 5 μm.

Additional DNA Analysis System Components. Using microfabrication processes compatible with the construction of the thermocapillary pump channels, a thermal cycling platform, a gel electrophoresis chamber, and a DNA detector were fabricated and tested. PCR thermal cycling was performed on a silicon substrate using heaters and temperature sensors from the same processed wafer as the thermocapillary pump. In this thermal reaction chamber device, a group of four closely spaced heater elements were tested to ensure compatibility with the standard PCR biochemical reactions. The device successfully amplified a single-copy sequence from total genomic mouse DNA in small aqueous drops (10–25 μl) placed on the processed silicon surface and covered with mineral oil to prevent evaporation (M.A.B. and B.F., unpublished data). However, variations in PCR amplification efficiency as large as 4-fold were observed between repetitions of the experiment.

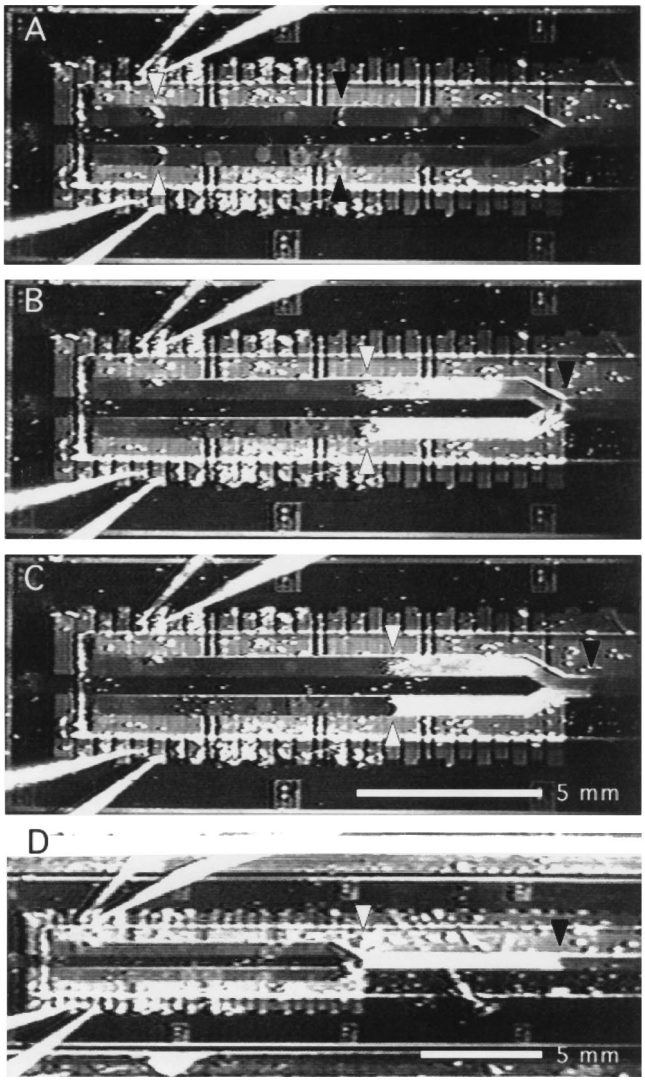

FIG. 4. Selected frames from a video showing drop motion and mixing in a Y-channel device. The device was constructed by bonding the silicon heater elements and glass channels shown in Fig. 3. The photographs are sampled at approximately 0.5-sec intervals and are as follows: (*A*) two 80-nl drops at their starting locations in the branches of the Y-channel, (*B*) initiation of movement by heating the left interface of both drops, (*C*) merging of the drops at the intersection, and (*D*) the combined drop. The open and filled arrowheads indicate the rear and leading meniscus for each drop, respectively.

Following PCR amplification or restriction enzyme digestion, DNA genotyping reactions are typically analyzed by gel electrophoresis. To demonstrate that standard DNA gel electrophoresis can operate in micron-sized channels identical to those used for drop motion, experiments were performed using etched glass channels bonded to planar quartz. Polyacrylamide gel electrophoresis of a fluorescently labeled DNA mixture is shown in a channel 500 μm wide and 25 μm deep (Fig. 5*B*). Separation of the component bands in a range of 100–1000 bp is clearly visible $<$1 mm from the buffer reservoir-to-gel interface. The high resolution of the detector (in this case, a conventional stereo microscope at $\times$10 magnification) allowed the use of an unusually short gel, and resolved several migrating bands.

Finally, integral DNA sensor elements were fabricated on the surface of silicon wafers to electronically detect migrating

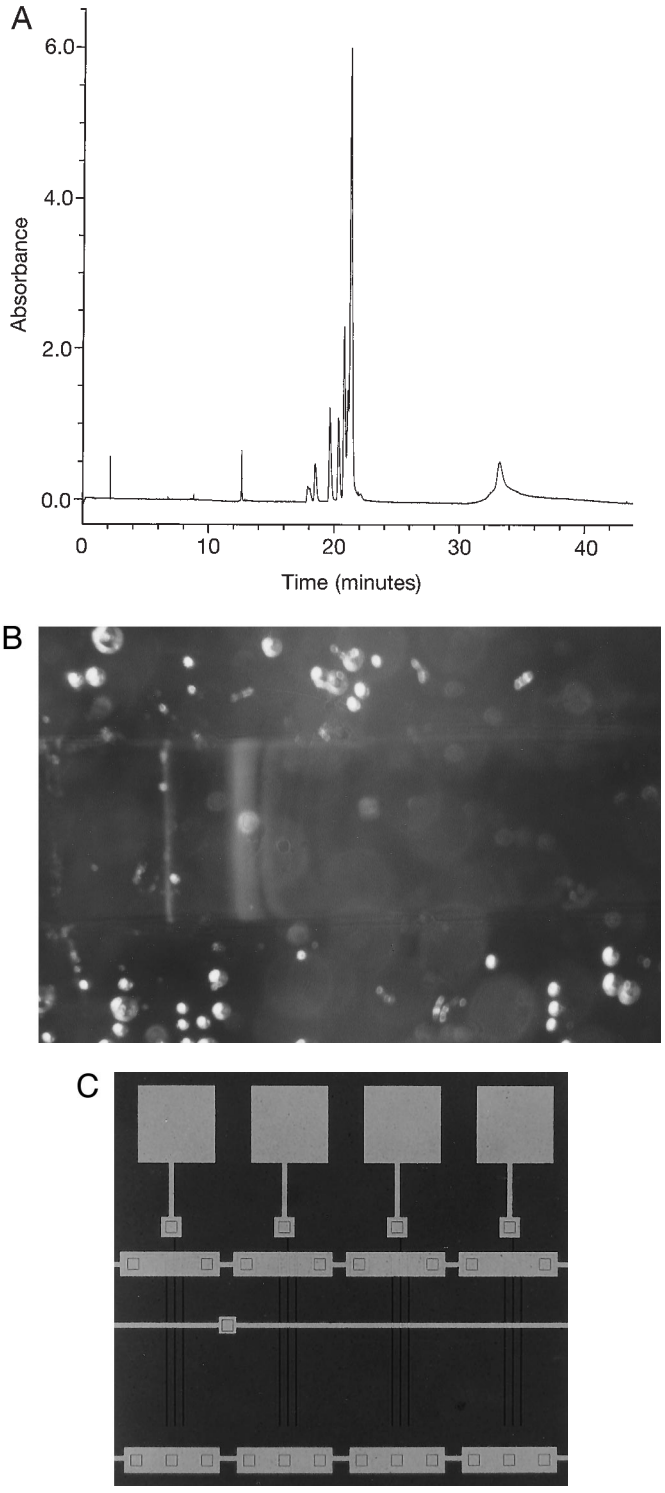

FIG. 5. Components for integrated DNA analysis. (*A*) Demonstration of a DNA restriction enzyme digestion in a microfabricated device identical to Fig. 4. The enzymatic reaction occurred by moving two drops (*Taq* I restriction enzyme and supercoiled plasmid) down separate channels using the thermocapillary technique, combining the drops, and heating the merged sample to 65°C in the channel. After the reaction, the sample was expressed from the microfabricated device and analyzed by conventional capillary gel electrophoresis. The electrophoretic chromatogram shows complete digestion products (elution time, 18–22 min) and minor residual undigested DNA (elution time, 34 min). (*B*) Photomicrograph of polyacrylamide gel electrophoresis in a 25-μm-deep by 500-μm-wide etched-glass channel identical to Fig. 3*A*. Electrophoresis was performed using a conventional polyacrylamide gel and buffer, with the positive electrode to the right and the DNA sample applied at the left. The light vertical line at the left is the gel-to-buffer interface. The digested plasmid DNA sample is labeled with intercalating dye YOYO-1 and visualized under incandescent light. The brightly staining bands correspond to DNA fragments in the 100- to 1000-bp size range. (*C*) Photomicrograph of a set of doped-diffusion diode elements fabricated in silicon which are able to detect β-particle events from ^{32}P-labeled aqueous DNA samples. For each diode element, the three parallel dark lines define the diffusion regions of the central detector and the guard ring shielding electrodes. The diffusion regions are $\approx$300 μm long and 4 μm wide.

DNA bands. A simple sensor capable of detecting decay events from radioactively labeled DNA can be fabricated on the surface of silicon wafers as a *p-n*-type diffusion diode (Fig. 5*C*). Radiation detection was chosen for the initial device since such diodes have a high sensitivity, small aperture dimensions, and well-known fabrication and response characteristics. Testing of the device with ^{32}P-labeled DNA demonstrates that it readily functions as a sensor capable of detecting single impacting events (C.H.M. and J.R.W., unpublished data). This diode, although currently configured for high-energy β particle detection, can also operate as a fluorescent light detector when combined with a matched fluorophore, wavelength filter, and excitation source.

DISCUSSION

The microfabricated elements in this report are capable of performing several processing steps in conventional DNA analysis. The individual elements have the potential for combination into a complete DNA genotype analysis processing path. No new biochemistries or DNA detection methods are required for their use; the components simply reproduce current laboratory procedures in a micron-sized environment. Each component was developed using only silicon or glass photolithographic production methods. As a consequence, all components retain the ability to be fabricated concurrently on the same substrate wafers. The use of common fabrication methods allows the assembly of increasingly complex, multicomponent, integrated systems from a small, defined set of standardized elements.

In particular, the thermocapillary pump mechanism is central to future integration efforts, for both DNA and other liquid-based analysis technologies. The pump system is easy to construct and control, using simple heating element wires and electronic sensors. Fine control of discrete drop location is only dependent on the density of individual heating elements along the channel. Detection of the drop location within the channel can be performed by using capacitors or conductive wires as sensors (M.A.B., T.S.S., and B.N.J., unpublished data). Because the pump mechanism requires no external force (other than application of heat), it should remain scalable within a wide range of integrated device sizes. Finally, because each droplet is moved uniquely, devices that incorporate branching pathways or parallel sample analysis present no inherent obstacle, other than requiring more complex electronic control circuitry.

Although the integration of individual components for drop motion and thermal reaction has been demonstrated in this report, significant design challenges will be faced in future component linkages. These include developments essential for connecting micron-scale devices with the macroscopic world, such as sample application, electronic control, and data acquisition. However, the linking of individual elements may benefit from the advantages of microfabricated silicon structures. For example, the resolving ability of DNA gel electrophoresis systems may be improved by the proximity and narrow width of silicon-based detectors placed immediately beneath the gel channel. Microfabricated diodes can be placed within 1 micron of the gel matrix and can have an aperture of 5

microns or less. Since the gel length required for the resolution of two migrating bands is proportional to the resolution of the detector, the incorporation of micron-width electronic detectors can significantly reduce the total gel length required for DNA analysis without sacrificing band-reading accuracy.

Future design efforts have a strong impetus to reduce component size and improve efficiency. The components in this report are simple and robust, but are not optimal for DNA analysis. Three areas of improvement are apparent: (*i*) increased detector sensitivity through the use of light-emitting DNA labels and wavelength-matched detectors, (*ii*) increased thermal control using Peltier-style heating/cooling elements, and (*iii*) incorporation of integrated silicon-based control circuitry. Regardless of specific component design, reductions in size will allow a higher packing density on a single fabricated wafer, leading to both more complex integrated systems and less expensive individual DNA analysis processors.

Specific predictions regarding the ultimate scale of miniaturization and cost of silicon-fabricated DNA analysis devices are premature. However, the foreseeable lower limit is constrained by DNA electrophoresis band detection. Currently, optical methods using efficient fluorophores can detect attomolar concentrations (corresponding to $\approx 10^5$ DNA molecules) migrating in capillary channels of 8×50 μm internal cross section (8). Reactions for synthesizing such DNA quantities can reasonably occur in 10 pl. An integrated system designed for picoliter volumes would require channel dimensions on the order of 10 $\mu m^2 \times 100$ μm (cross section $\times$ length). At this size, thousands of individual devices would occupy a single 100-mm-diameter wafer. In the configuration described in this report, a single wafer is estimated to cost $5000; however, processing costs are significantly reduced when large numbers of wafers are fabricated simultaneously.

The significant investment in photolithographic production technologies spurred by the microprocessor industry provides a format for further advances in integrated micron-scale DNA analysis devices. The production of silicon microfabricated devices can occur in mass quantities and at low incremental unit cost (11, 26, 27). Consequently, while the reduction in DNA sample volume and scale of these devices will provide some advantage, of equal importance will be the economic savings from inexpensive batch fabrication methods. In the same way that photolithographic silicon fabrication has reduced the cost and improved the portability of electronic systems over the past three decades, the use of silicon technology may have a significant impact on the practical application of DNA analysis.

We thank Dr. K. Wise and the staff of the Solid State Electronics Laboratory at the University of Michigan Department of Electrical Engineering and Computer Science for their assistance in wafer fabrication; Drs. Y. Boyd and K. Calame for the sequence of the *Tfe3* specific primers; Dr. C. Cain for his encouragement in forming this collaboration; and the University of Michigan Office of the Vice President for Research, the College of Engineering, the Associate Dean for Research of the Medical School, and the University of Michigan Genome Center for support through developmental funds. The project receives grant support from the National Institutes of Health (Grant R01-HG01044). D.T.B. is a recipient of support from the Searle Scholars Program of the Chicago Community Trust. [Computer files for generating the fabrication masks and for the computer instrumentation controls are available from the authors on request.]

1. Gyapay, G., Morissette, J., Vignal, A., Dib, C., Fizames, C., Millasseau, P., Marc, S., Bernardi, G., Lathrop, M. & Weissenbach, J. (1994) *Nat. Genet.* **7,** 246–339.
2. Dietrich, W. F., Miller, J. C., Steen, R. G., Merchant, M., Damron, D., Nahf, R., Gross, A., Joyce, D. C., Wessel, M., Dredge, R. D., Marquis, A., Stein, L. D., Goodman, N., Page, D. C. & Lander, E. S. (1994) *Nat. Genet.* **7,** 220–245.
3. Fleischmann, R. D., Adams, M. D., White, O., Clayton, R. A., Kirkness, E. F. *et al*. (1995) *Science* **269,** 496–512.
4. Mullis, K. B. & Faloona, F. (1987) *Methods Enzymol.* **155,** 335–350.
5. Nickerson, D. A., Kaiser, R., Lappin, S., Stewart, J., Hood, L. & Landegren, U. (1990) *Proc. Natl. Acad. Sci. USA* **87,** 8923–8927.
6. Weber, J. L. & May, P. E. (1989) *Am. J. Hum. Genet.* **44,** 388–396.
7. Todd, J. A. (1995) *Proc. Natl. Acad. Sci. USA* **92,** 8560–8565.
8. Woolley, A. T. & Mathies, R. A. (1994) *Proc. Natl. Acad. Sci. USA* **91,** 11348–11352.
9. Northrup, M. A., Ching, M. T., White, R. M. & Watson, R. T. (1993) *Digest of Technical Papers: Transducers 1993* (IEEE, New York), pp. 924–926.
10. Effenhauser, C. S., Paulus, A., Manz, A. & Widmer, H. M. (1994) *Anal. Chem.* **66,** 2949–2953.
11. Petersen, K. E. (1982) *IEEE Proc.* **70,** 420–457.
12. Gravensen, P., Branebjerg, J. & Jensen, O. S. (1993) *J. Micromech. Microeng.* **3,** 168–182.
13. Manz, A., Effenhauser, C. S., Burggraf, N., Harrison, D. J., Seiler, K. & Fluri, K. (1994) *J. Micromech. Microeng.* **4,** 257–265.
14. Colgate, J. E. & Matsumoto, H. (1990) *J. Vac. Sci. Technol.* **8,** 3625–3633.
15. Wilding, P., Shoffner, M. A. & Kricka, L. J. (1994) *Clin. Chem.* **40,** 1815–1818.
16. Harrison, D. J., Fluri, K., Seiler, K., Fan, Z., Effenhauser, C. S. & Manz, A. (1993) *Science* **261,** 895–897.
17. Manz, A., Harrison, D. J., Verpoorte, E. M. J., Fettinger, J. C., Paulus, A., Lüdi, H. & Widmer, H. M. (1992) *J. Chromatogr.* **593,** 253–258.
18. Jacobson, S. C., Hergenröder, R., Koutny, L. B. & Ramsey, J. M. (1994) *Anal. Chem.* **66,** 2369–2373.
19. Schoonevald, E. M., Audet, S. A., van Eijk, C. W. E., Gelsema, S. J., Hollander, R. W. & Wouters, S. E. (1991) *Nuclear Instr. Methods Phys. Res.* **A305,** 581–586.
20. Van den Berg, A. & Bergveld, P. eds, (1995) *MESA Monograph: Micro Total Analysis Systems* (Kluwer, Boston).
21. Arnheim, N. & Erlich, H. (1992) *Annu. Rev. Biochem.* **61,** 131–156.
22. Roman, C., Matera, A. G., Cooper, C., Artandi, S., Blain, S., Ward, D. C. & Calame, K. (1992) *Mol. Cell. Biol.* **12,** 817–827.
23. Probstein, R. F. (1989) *Physicochemical Hydrodynamics* (Butterworths, Boston).
24. Tenan, M. A., Hackwood, S. & Beni, G. (1982) *J. Appl. Phys.* **53,** 6687–6692.
25. Dussan, E. B. V. (1979) *Annu. Rev. Fluid Mech.* **11,** 371–399.
26. Wolf, S. & Tauber, R. N. (1986) *Silicon Processing for the VLSI Era* (Lattice, Sunset Beach, CA), Vol. 1.
27. Jaeger, R. C. (1993) *Introduction to Microelectronic Fabrication* (Addison–Wesley, New York), Vol. 5.